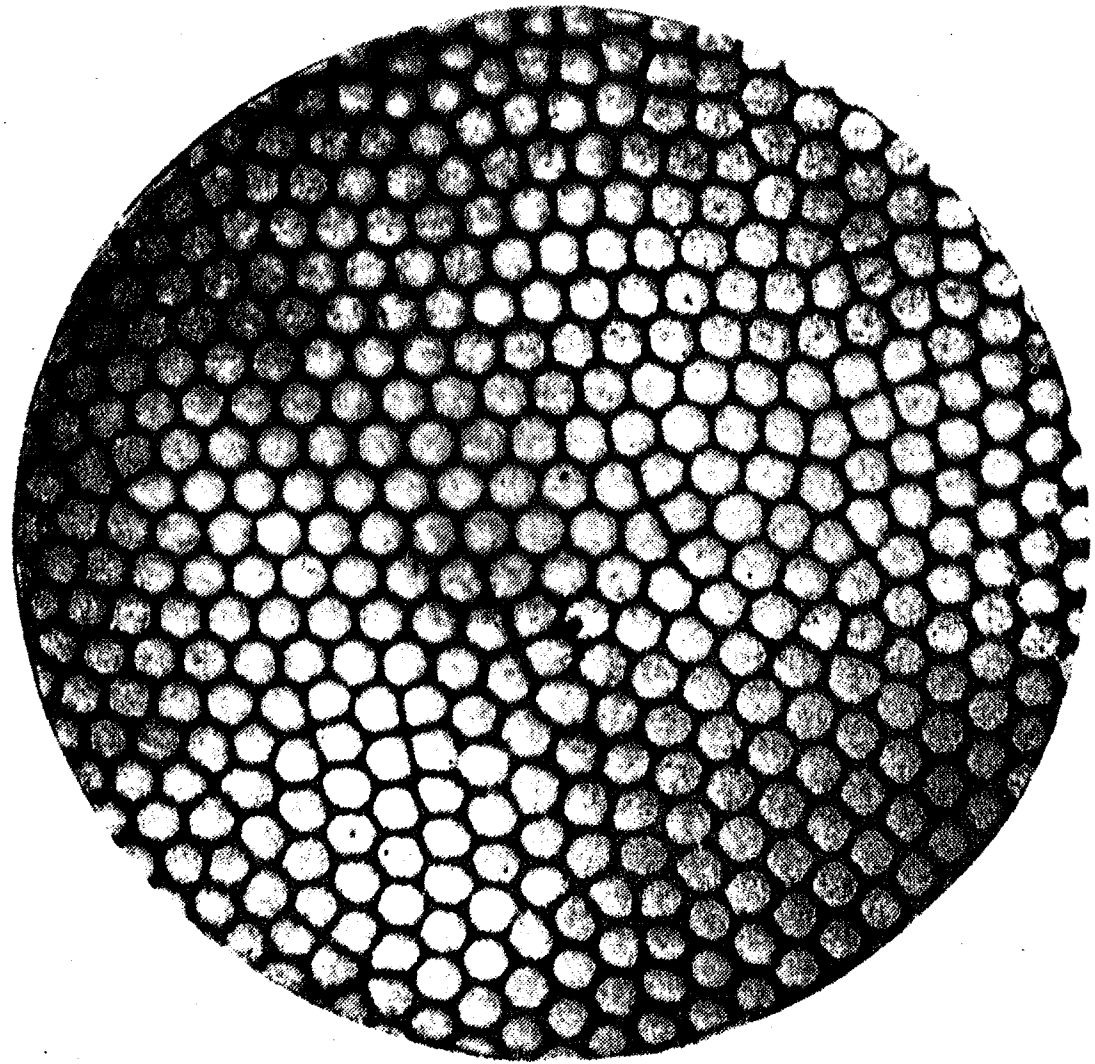

Fig. 3.1 Bénard cells in spermaceti. A reproduction of one of Bénard's original photographs from Chandrasekhar (1961).

The simplest solution is that of horizontal rolls for which, if they are aligned in the x direction, $k_x = 0$. Then

$$w = w_1(z) \cos k_c y. \tag{3.1.30}$$

The horizontal velocity components may be obtained by first noticing that the vorticity of the flow about a vertical axis is always zero. From (3.1.6) and (3.1.7) we have

$$\left(\frac{\partial}{\partial t} - \nu\nabla^2\right)\left(\frac{\partial v}{\partial x} - \frac{\partial u}{\partial y}\right) = 0.$$

For all boundary types, the solution of the above is

$$\frac{\partial v}{\partial x} - \frac{\partial u}{\partial y} = 0.$$

Since the flow is irrotational, we may express the horizontal velocity components in terms of a velocity potential ϕ:

$$u \equiv \frac{\partial \phi}{\partial x}, \qquad v \equiv \frac{\partial \phi}{\partial y},$$

and from the continuity equation,

$$\frac{\partial^2 \phi}{\partial x^2} + \frac{\partial^2 \phi}{\partial y^2} = -k^2 \phi_1 = -\frac{dw_1}{dz}, \tag{3.1.31}$$

where we have let $\phi = \phi_1 \exp(ik_x x + ik_y y)$.

The solution for the horizontal velocity components corresponding to (3.1.30) is

$$v = -\frac{1}{k_c}\frac{dw_1}{dz}\sin k_c y,$$

$$u = 0.$$

The buoyancy field may be derived using (3.1.12):

$$B = \frac{\nu}{k_c^2}\left(\frac{d^2}{dz^2} - k_c^2\right)^2 w_1 \exp\left[ik_c y\right].$$

Similarly, the pressure distribution at the onset of instability can be obtained through (3.1.11):

$$\frac{p}{\rho_0} = \frac{\nu}{k_c^2}\left(\frac{d^2}{dz^2} - k_c^2\right)\frac{dw_1}{dz^2}\exp\left[ik_c y\right].$$

Both the buoyancy and pressure fields are horizontally in phase with the vertical motion. For the roll solution, then, we have two-dimensional circulations with no velocity component along the roll axes, and with low pressure underneath and high pressure above the warm ascending branch; the converse is true for the descending branch. In summary,

$$
\begin{aligned}
w &= w_1(z)\cos k_c y, \\
v &= -\frac{1}{k_c}\frac{dw_1}{dz}\sin k_c y, \\
u &= 0, \\
B &= \frac{\nu}{k_c^2}\left(\frac{d^2}{dz^2} - k_c^2\right)^2 w_1 \cos k_c y, \\
\frac{p}{\rho_0} &= \frac{\nu}{k_c^2}\left(\frac{d^2}{dz^2} - k_c^2\right)\frac{dw_1}{dz}\cos k_c y,
\end{aligned}
$$

for horizontal rolls aligned in the x direction.

Table 3.1 The critical Rayleigh numbers and horizontal wavenumbers for the onset of instability in a fluid confined between parallel plates

Type of boundary	R_{ac}	k_c	$\pi/k_c \left(= \frac{1}{2} L_c\right)$
Both free	657.5	2.22	1.42
One rigid and one free	1100.7	2.68	1.17
Both rigid	1707.8	3.12	1.01

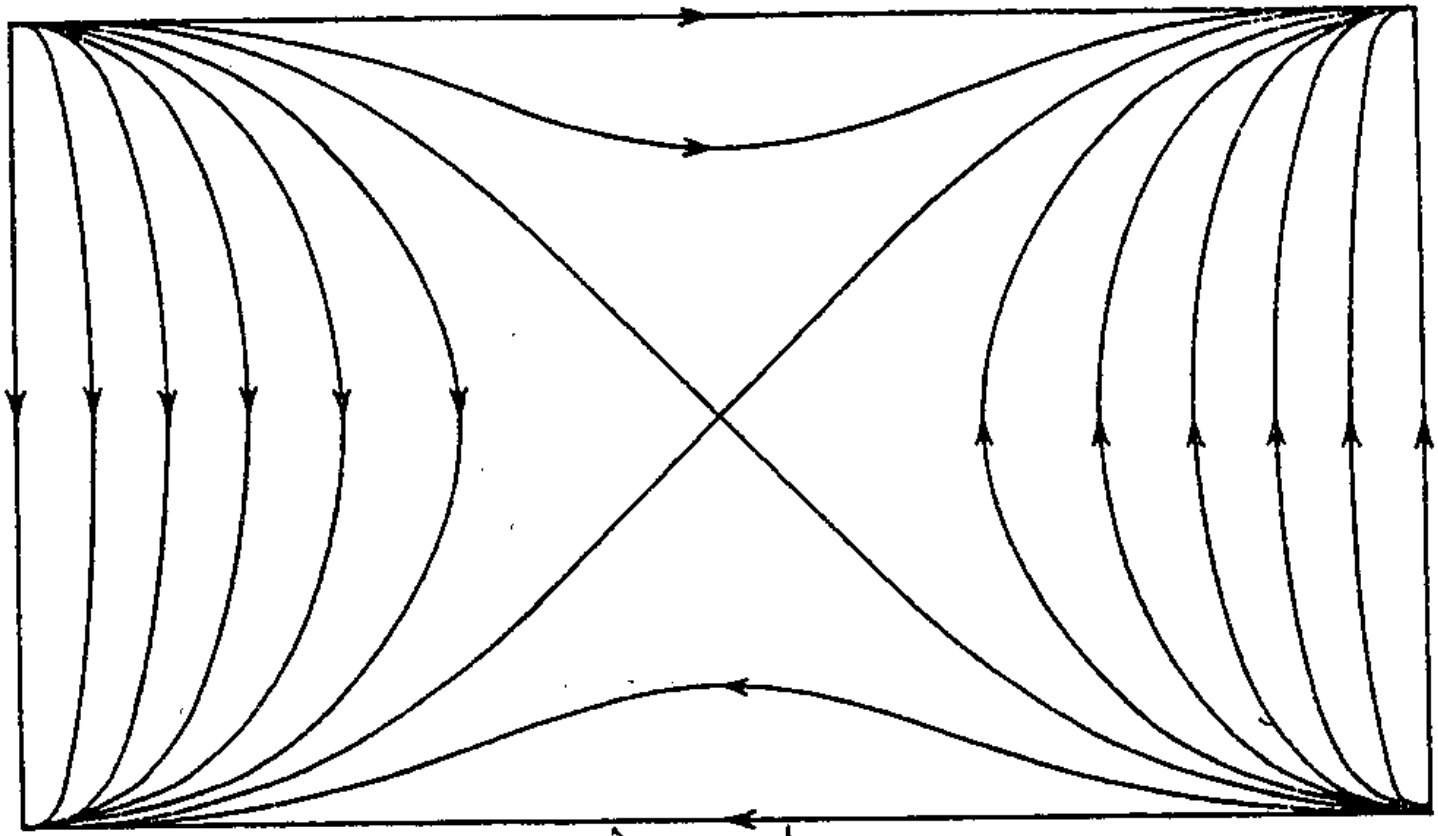

Fig. 3.2 Streamlines in a horizontal plane for a rectangular cell. [*From Chandrasekhar (1961).*]

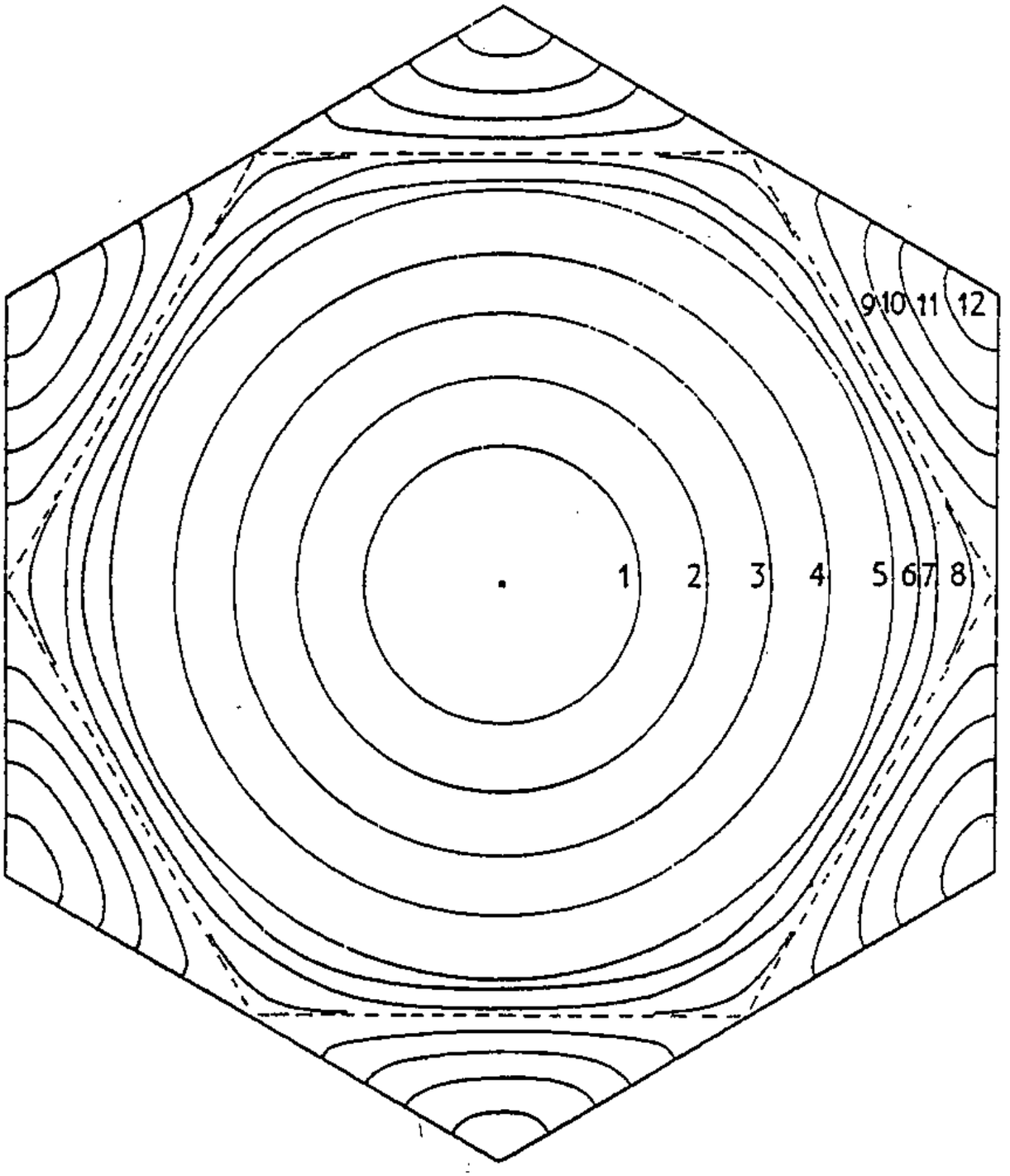

Fig. 3.3 Contours of constant w in a hexagonal cell. The contour labels 1 to 12 correspond to relative vertical velocities of 0.75, 0.50, 0.25, 0, −0.20, −0.25, −0.30, −0.325, −0.36, −0.40, −0.44, and −0.48. The value of w on the inscribed hexagon (shown in dashed lines) is $-\frac{1}{3}$, and at the vertices of the bounding hexagon it has the value $-\frac{1}{2}$. The streamlines in this plane are orthogonal to the w contours. [*From Chandrasekhar (1961).*]

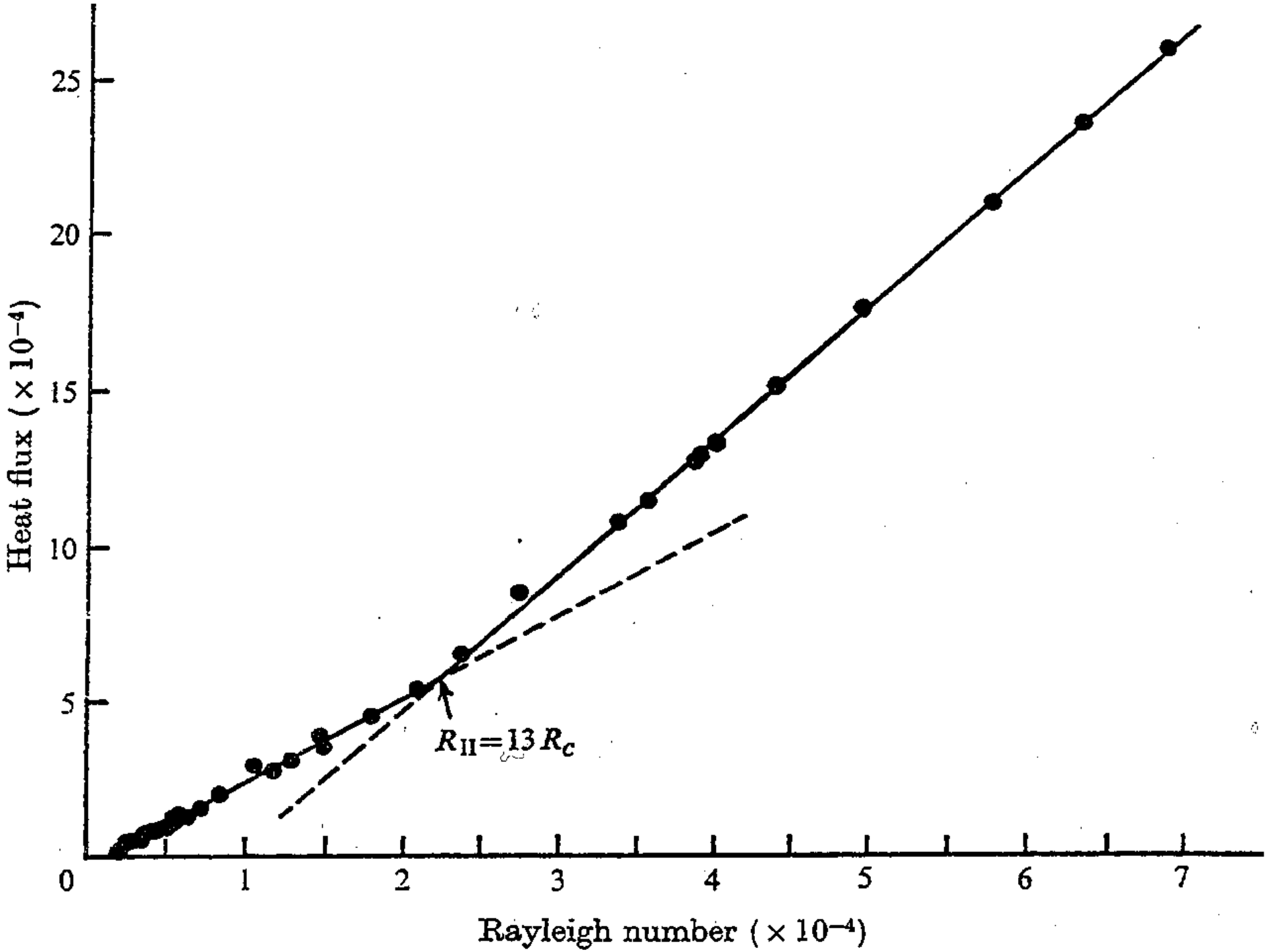

Fig. 3.11 Nusselt number (heat flux) plotted against Rayleigh number, for Prandtl number 100, from the laboratory experiments of Krishnamurti (1970a).

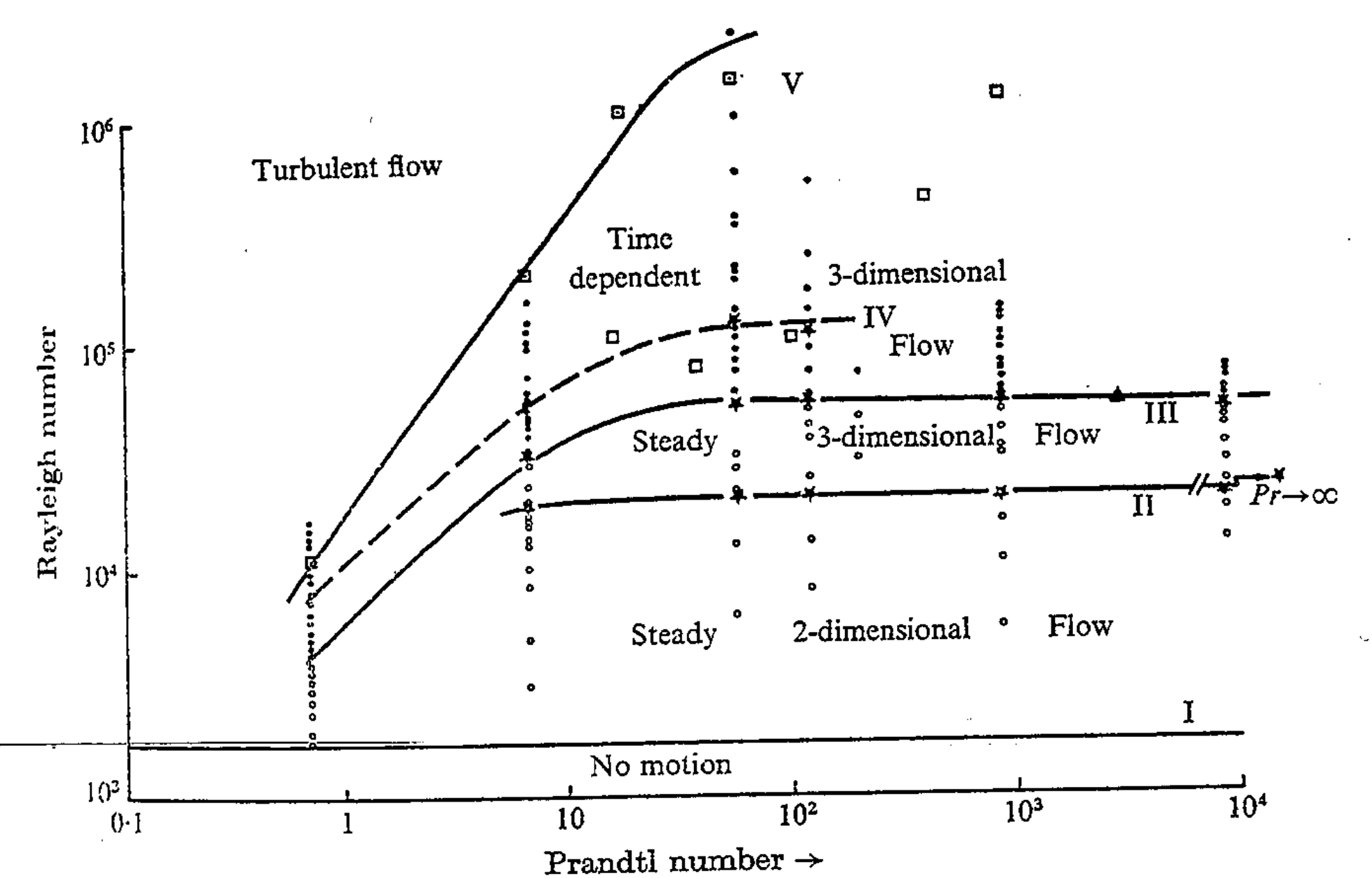

Fig. 3.12 Regime diagram for experiments on Rayleigh convection. Circles represent steady flows and circular dots denote time-dependent convection. The stars represent transition points. The open squares show independent laboratory observations of time-dependent flow by Rossby (1966) and the squares with a dot in the center show observations of turbulent flow by Willis and Deardorff (1967). [*From Krishnamurti (1970b).*]

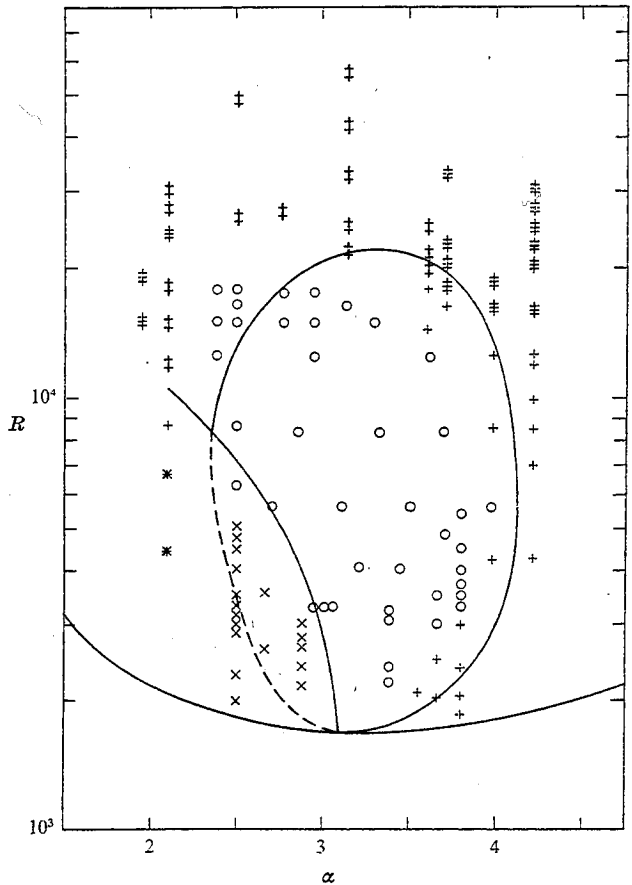

Fig. 3.13 Experimental results of Busse and Whitehead (1971) plotted on theoretical regime diagram of Busse (1967). The figure shows the Rayleigh number, plotted against horizontal wavenumber. The solid curve at bottom is the critical Rayleigh number, while the left and right curves represent the stability boundaries for zigzag and cross-roll instability, respectively. The open circles show observations of steady roll circulation, x's show zigzag instability, +'s denote cross-roll instability leading to rolls, ‡'s show cross-roll instability leading to bimodal convection, and ≠'s show cross-roll instability leading to transient rolls.

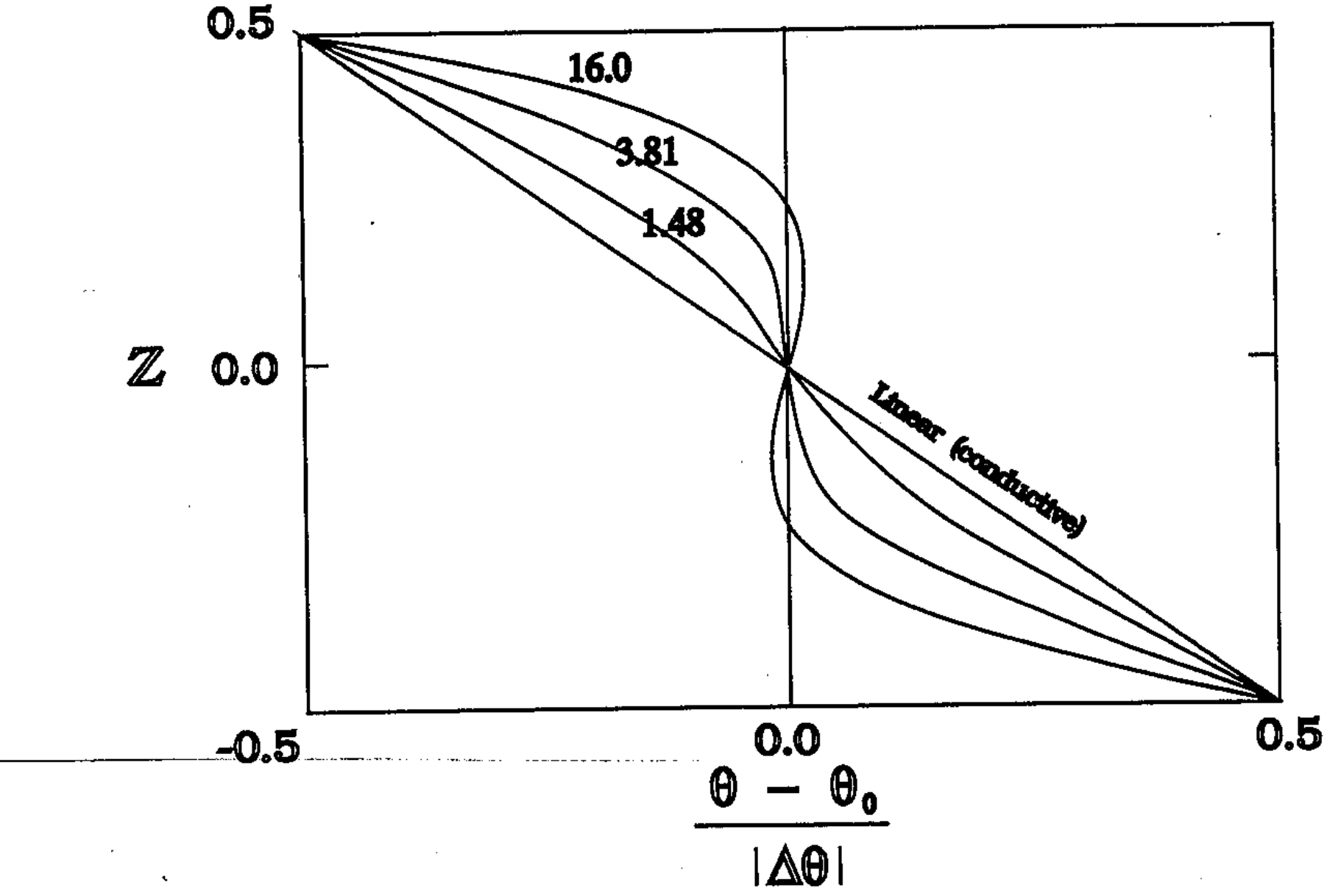

Fig. 3.14 Observed mean temperature profiles in a convecting layer. Curves are labelled with the value of R_a/R_{ac}. [*From Gille (1967).*]

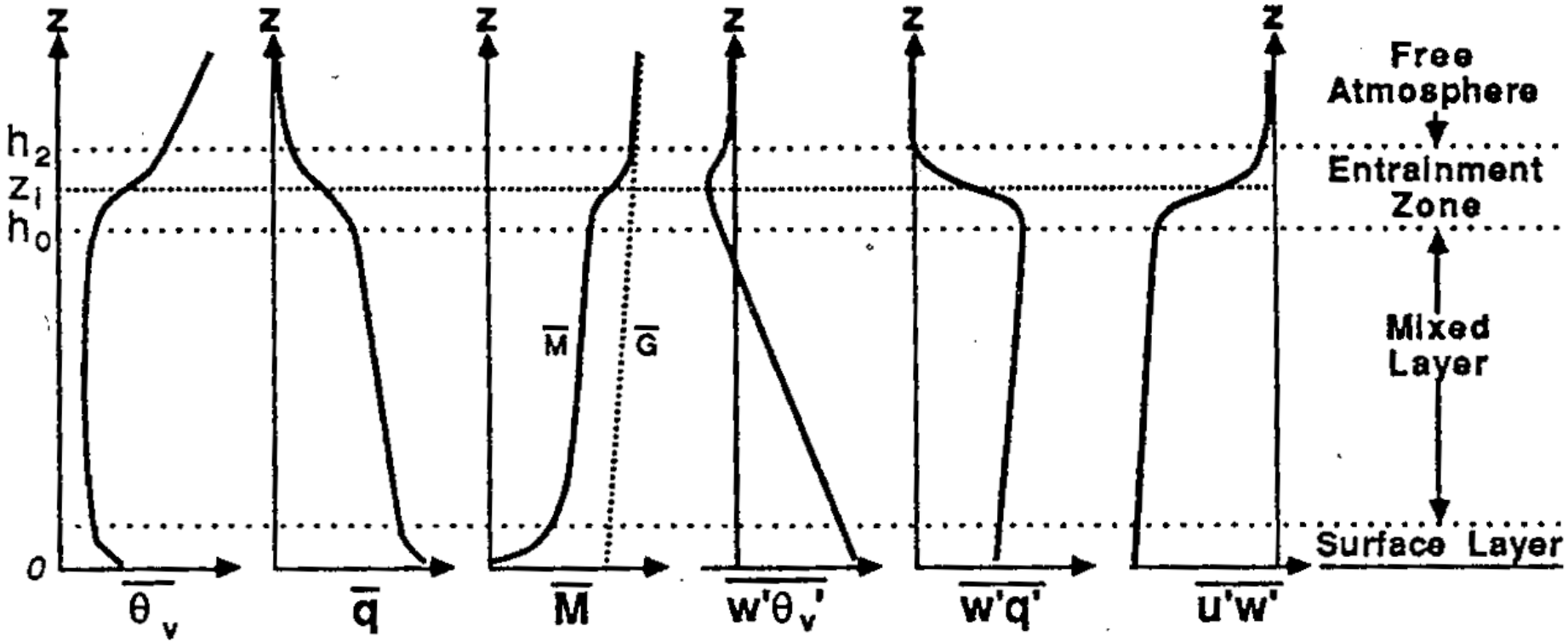

Fig. 3.16 Typical profiles of quantities in a convective boundary layer. The quantities are mean virtual potential temperature ($\overline{\theta}_v$), specific humidity ($\overline{q}$), wind speed ($\overline{M}$), buoyancy flux ($\overline{w'\theta'_v}$), humidity flux ($\overline{w'q'}$), and momentum flux ($\overline{u'w'}$). [*From Stull (1988).*]